# The Landscape of Immune Cell Infiltration in the Glomerulus of Diabetic Nephropathy: Evidence Based on Bioinformatics

**Wei ZHOU**
Department of Clinical Pharmacy, The Second Affiliated Hospital, Guangzhou University of Chinese Medicine https://orcid.org/0000-0003-4242-7187

**Yaoyu LIU**
Department of Clinical Pharmacy, The Second Affiliated Hospital, Guangzhou University of Chinese Medicine

**Qinghong HU**
Department of Clinical Pharmacy, The Second Affiliated Hospital, Guangzhou University of Chinese Medicine

**Jiuyao ZHOU**
Department of Pharmacology, School of Pharmaceutical Sciences, Guangzhou University of Chinese Medicine

**Hua LIN** ( lh33895380@163.com )
Department of Clinical Pharmacy, The Second Affiliated Hospital, Guangzhou University of Chinese Medicine

**Research Article**

**Keywords:** Diabetic nephropathy, Immune cell infiltration, CIBERSORT, Bioinformatics

**Posted Date:** June 1st, 2021

**DOI:** https://doi.org/10.21203/rs.3.rs-554679/v1

# Abstract

Background

Increasing evidence suggests that immune cell infiltration contributes to the pathogenesis and progression of diabetic nephropathy (DN). We aim to unveil the immune infiltration pattern in the glomerulus of DN and provide potential targets for immunotherapy.

Methods

Infiltrating percentage of 22 types of immune cell in the glomerulus tissues were estimated by the CIBERSORT algorithm based on three transcriptome datasets mined from the GEO database. Differentially expressed genes (DEGs) were identified by the “limma” package. Then immune-related DEGs were identified by intersecting DEGs with immune-related genes (downloaded from Immport database). The protein-protein interactions of Immune-related DEGs were explored using the STRING database and visualized by Cytoscape. The enrichment analyses for KEGG pathways and GO terms were carried out by the gene set enrichment analysis (GSEA) method.

Results

9 types of immune cell were revealed to be significantly altered in the glomerulus tissues of DN (Up: B cells memory, T cells CD4 naive, Macrophages M2, Dendritic cells resting, Mast cells resting, Mast cells activated; Down: NK cells resting, Monocytes, Neutrophils). Correlation analysis revealed that immune infiltration act as a complicated and tightly regulated network, among which T cells gamma delta and T cells CD4 naive show the most synergistic effect ($r = 0.58$, $p < 0.001$); meanwhile, T cells CD8 and T cells CD4 memory resting show the most competitive effect ($r = -0.67$, $p < 0.001$). Several pathways related to immune were significantly activated. Moreover, 6 hub genes with a medium to strong correlation with renal function (eGFR) were identified (ALB, EGF, FOS, CXCR1, CXCR2, CCL2).

Conclusion

In the glomerulus of DN, the immune infiltration pattern changed significantly. A complicated and tightly regulated network of immune cells exists in the pathological of DN. The hub genes identified here will facilitate the development of immunotherapy.


# Background

Diabetic nephropathy (DN) is an extremely common complication of diabetes mellitus, affecting up to 30% of individuals with type 1 diabetes mellitus and 40% of individuals with type 2 diabetes mellitus[1]. Over the last two decades, no new drugs have been approved to specifically prevent DN or to improve kidney function[2]. Current strategies to treat this disease mainly focus on intensification control of glycemic, blood pressure and other risk factors [3]. But a significant proportion of patients still progress to

end stage renal failure overtime with a well control of risk factors, which highlight the urgent need to identify effective therapies.

Recently, DN is increasingly considered as an inflammatory disease, with immune modulation being involved in every stage. Immune cells infiltrated in kidney tissues, such as macrophages, T cells, and mast cells produce various inflammatory cytokines, metalloproteinases, and growth factors, which modulate the local response and increase inflammation [4–8].

Although there is substantial evidence for the vital roles of macrophages, T cells, B cells, and mast cells, the effect of other immune cells including neutrophils, plasma cells, and dendritic cells are less clear. Furthermore, the immune system contains various types of immune cell, which constitute a complex regulatory network, potential intercorrelations of them in the pathological process of DN are less clear. Therefore, an integrated analysis of immune infiltration, differentially expressed genes, and aberrant pathways activation in kidney tissues is essential.

Here, we used the CIBERSORT algorithm to analyse the abundance of 22 kinds of immune cells in the glomerulus samples of DN based on three microarray datasets mined from the Gene Expression Omnibus (GEO)[9]. Then an integrated bioinformatics analysis was conducted to screen immune-related differentially expressed genes(IR-DEGs)and explore aberrant pathways activation. Besides, we evaluated the correlation between IR-DEGs with immune infiltration cells and clinical indicator. Our research provides a potential value for immunotherapy of DN.

## Materials And Methods

# Data acquisition

We systematically searched publicly available DN gene expression datasets on Gene Expression Omnibus (GEO) database using the following terms: (“DN” or “DKD” or “diabetic nephropathy” or “diabetic kidney disease”) and “Homo sapiens” [porgn:_txid9606] and (“Expression profiling by array”[Filter] or “Expression profiling by high throughput sequencing”[Filter]).

Datasets included in this study have to meet the following criteria: (1) The organism of samples is Homo sapiens. (2) The sample type is glomerular tissue. (3) gene expression was detected by microarray or high-throughput sequencing. (4) dataset including DN and NC (negative control) samples (5) The dataset contains more than 3 samples per group. Finally, three datasets were included in this research (GSE96804, GSE30528, and GSE1009). Database searches were conducted in February 2021. The detailed workflow of this study is shown in Fig. 1.

# Data pre-processing

The probe ID was converted to a gene symbol using the platform annotation files. If a gene matched multiple probes, the maximum value of multiple probes expression was applied. To avoid sample

heterogeneity arising from different technical platforms and dissimilar methods of processing data, batch effect removal and normalization were conducted by the “limma” package[10, 11]. Then Principal component analysis (PCA) was performed to Confirm homogeneity after data pre-processing.

# Immune cell infiltration Profiling

A deconvolution algorithm—CIBERSORT—was used to estimate the relative proportion of 22 types of infiltrating immune cell in glomerular tissue by identifying 547 immune cell-related genes[9].

The normalized gene expression data were uploaded to the CIBERSORT web portal (http://CIBERSORT.stanford.edu/) with a parameter of 1000 permutation and a relative mode. $P < 0.05$ was considered to be statistically significant. The Pearson correlation coefficient between each immune cell was calculated and visualized with a correlation heatmap by the “corrplot” package.

# Differentially expressed gene analysis

The “limma” package was used to reveal the differentially expressed genes (DEGs) between DN and NC samples with a threshold of |log2FC (fold change) | > 1 and adjusted P-value < 0.05[11]. The visualization of DEGs was conducted by the “ComplexHeatmap” and “ggplot2” packages.

# Gene set enrichment analysis (GSEA)

The enrichment analyses for Gene Ontology (GO) terms and Kyoto Encyclopaedia of Genes and Genomes (KEGG) pathways were carried out by the gene set enrichment analysis (GSEA) method with the “clusterProfiler” package.

# Protein-protein interaction (PPI) analysis of Immune-related DEGs

The immune-related gene list was downloaded from the ImmPort Database (https://www.immport.org/shared/home). Then immune-related differentially expressed genes (Immune-related DEGs) were identified by intersecting DEGs with immune-related genes. The protein-protein interactions of Immune-related DEGs were estimated by the Search Tool for the Retrieval of Interacting Genes (STRING) database (http://string-db.org). Then genes with a confidence score of interaction more than 0.95 were visualized by Cytoscape (version 3.8.2). The Maximum clique centrality (MCC) algorithm of the “Cytohubba” plug-in was used to identify Hub genes[12].

# Correlation analysis of Hub genes with infiltrated immune cells and clinical indicator

Correlation analysis between hub genes and immune cells were calculated and visualized with the “corrplot” package. Then the hub genes which has a medium to strong correlation with immune cells were conducted correlation analysis with renal function indicator—eGFR—by the Nephroseq database (version v5) and visualized with the “ggpubr” package.

# Statistical Analysis

All statistical analysis was performed on R software (version 4.0.2). An independent t-test was performed to compare continuous variables between two groups, p-value < 0.05 was considered statistically significant. Correlations were assessed by the Pearson correlation coefficient (0.1 | r | 0.4 represents a weak correlation; 0.4 | r | 0.7 represents a medium correlation; and | r | 0.7 represents a strong correlation).

## Results

# Data Integration and Removal of Batch Effects

First, the GEO series of GSE96804 (41 DN and 20 NC samples), GSE30528 (9 DN and 13 NC samples), and GSE1009(3DN and 3 NC samples) were acquired from the GEO database and merged as one big dataset with a total of 89 samples (53 DN and 36 NC samples). Second, the batch effect was evaluated and visualized by a box plot and a PCA score plot (Fig. 2A-B). Then batch effect removement and data normalization were conducted with the “limma” package. At last, the homogeneity between GEO series was confirmed (Fig. 2C-D).

# Infiltration Proportion of Immune Cells Changed in DN group

The proportion of 22 types of immune cells in the glomerulus tissues were estimated by the CIBERSORT algorithm. As shown in Fig. 3A, the fraction of immune cells varied significantly among the samples and groups. Due to the limitations of the CIBERSORT algorithm, the infiltration of some low abundance immune cell subsets wasn’t fully revealed. The violin plot shows that 9 types of cells changed significantly in DN. Among which, 6 types were up-regulated and 3 types were down-regulated (Fig. 3B). These results demonstrated that there were different infiltration patterns of immune cells in DN glomerular tissues.

To evaluate whether different types of immune cells interact with each other during infiltration, correlation analysis was conducted. And we found multiple pairs of positively or negatively related immune cells. Among them, T cells gamma delta and T cells CD4 naive show the most synergistic effect ($r = 0.58$, $p < 0.001$); meanwhile, T cells CD8 and T cells CD4 memory resting show the most competitive effect ($r = -0.67$, $p < 0.001$) (Fig. 4). Collectively, these results indicate that immune cells may not infiltrate individually but act as a complicated and tightly regulated network in the pathological of DN.

# Identification of differentially expressed genes(DEGs)

In differential expression analysis (53 DN vs. 36 NC), a total of 149 differentially expressed genes were identified, of which 57 were upregulated and 92 were downregulated in DN. To visualize the DEGs more intuitively, we plotted a volcano plot and a heatmap plot (Fig. 5A-B). The expression details of the top 10 upregulated and top 10 downregulated genes are listed in Table 1.

Table 1
The top 10 upregulated and top 10 downregulated genes identified by differential gene expression analysis.

| Symbol | $log_2FC$ | AveExpr | p.Value | adj.P.Val | Change |
|---|---|---|---|---|---|
| DUSP1 | -1.372 | 6.621 | 1.77E-19 | 1.49E-15 | down |
| FOS | -2.750 | 5.014 | 2.65E-16 | 1.12E-12 | down |
| NFIL3 | -1.121 | 4.647 | 4.7E-15 | 1.25E-11 | down |
| WT1-AS | -1.169 | 5.584 | 5.92E-15 | 1.25E-11 | down |
| DPP6 | -1.765 | 5.990 | 1.95E-14 | 2.74E-11 | down |
| PRKAR2B | -1.628 | 5.746 | 3.11E-14 | 3.28E-11 | down |
| LPL | -1.560 | 5.521 | 4.06E-14 | 3.43E-11 | down |
| CXCR1 | -1.317 | 4.508 | 1.64E-13 | 1.19E-10 | down |
| ZFP36 | -2.173 | 7.294 | 1.81E-13 | 1.19E-10 | down |
| CXCR2 | -1.234 | 5.107 | 1.9E-13 | 1.19E-10 | down |
| NAIP | 1.051 | 5.123 | 5.58E-12 | 1.21E-09 | up |
| GPR18 | 1.112 | 4.938 | 5.48E-11 | 7.33E-09 | up |
| COL1A2 | 1.766 | 5.151 | 1.04E-10 | 1.17E-08 | up |
| LUM | 2.727 | 5.328 | 2.47E-10 | 2.3E-08 | up |
| IGFBP6 | 1.135 | 5.141 | 3.08E-10 | 2.77E-08 | up |
| PLK2 | 1.020 | 5.883 | 1.19E-09 | 7.49E-08 | up |
| COL6A3 | 1.531 | 4.784 | 3.36E-09 | 1.84E-07 | up |
| MOXD1 | 1.924 | 4.667 | 3.86E-09 | 2.01E-07 | up |
| SOX4 | 1.014 | 5.959 | 5.95E-09 | 2.87E-07 | up |
| MARCKS | 1.491 | 6.194 | 7.69E-09 | 3.46E-07 | up |

# Gene set enrichment analysis (GSEA)

To explore the possible pathways and gene sets associated with immune functions, we performed GSEA. Results show that several pathways related to immune, diabetes, and Kidney disease were significantly activated in the DN group, including-Chemokine signalling pathway, Cytokine – cytokine receptor interaction, and Renin secretion etc. (Fig. 6A-B).

To explore the immune-related gene function in the pathological of DN, GO biological processes (GO-BP) analysis was conducted using GSEA. Eight representative immune-related biological processes were

shown in Fig. 6C-D. These results show that immune related processes had been activated aberrantly in the glomerulus of DN.

# PPI network construction of Immune-related DEGs

Thirty-nine immune-related differentially expressed genes were obtained by intersecting DEGs with the lists of immune-related genes (IRGs) obtained from the ImmPort database (Fig. 6A). To get a further understanding of the regulation effects among these genes, a PPI (Protein-protein interaction) was constructed by the “Cytoscape” (Fig. 6B), and ten hub genes were identified by the Maximum clique centrality (MCC) algorithm using “Cytohubba” plug-in (Fig. 6C).

# Correlation analysis between Hub genes and infiltrated immune cells

To understand the molecular mechanisms of alteration in infiltrating immune cells in detail, the correlations between immune related hub genes and immune cells need to be unveiled. So, we calculated Pearson's correlation coefficient for hub genes with differentially infiltrated immune cells. Figure 8A demonstrates that 7 of the 10 hub genes have moderate to high correlations with differential infiltrated cells($r > 0.4$), Especially CXCR2 with neutrophils ($r = 0.85$).

# Exploration of the association between hub genes and clinical indicator

Furthermore, we explored the correlations between the 7 hub genes and the vital clinical renal function indicator—eGFR—based on the Nephroseq database (version: v5). The data show that 3 genes are positively correlated with eGFR levels, 3 genes are negatively correlated with eGFR levels, only the gene PTGS2 has no obvious correlation with eGFR (Fig. 8B-H).

## Discussion

With the advancement of bioinformatics, efficient algorithms have accelerated the transition of various omics big data to new therapeutic targets. As one of the most robust algorithms for analyzing immune cell infiltration—CIBERSORT—has been used in multiple tissues[13–15]. In this study, we used it to explore the landscape of immune infiltration in the glomerulus of DN.

In summary, we found that a variety types of infiltrated immune cell have altered during the pathogenesis of DN. Correlation analysis shows that the immune response may act as a complicated and tightly regulated network. In addition, we also screened out 6 immune-related hub genes which not only have correlations with differently infiltrated immune cells but also have a medium to strong correlation with eGFR (the most important renal function indicators).

Boris B. Betz performed urinary peptidomics analysis in a rodent DN model and found that urinary epidermal growth factor (EGF) was more than 2-fold reduced in rats with DN in comparison with

controls[16]. CXCR1 and CXCR2 are two cell-surface G protein-coupled receptors, CXCL8 binds to them for recruiting neutrophil and initiating inflammation in DN[17].In our study, we found that CXCR1 and CXCR2 have a strong correlation with neutrophil infiltration (r = 0.79 and 0.85). The chemokine C-C Motif Chemokine Ligand 2 (CCL2), also referred to as monocyte chemoattractant protein 1, is ubiquitously expressed in various cell types and is responded to a wide variety of stimulation[18]. The CCL2 knockout mice caused reduced macrophage accumulation in the kidney and the progression of renal injury in diabetic conditions[19]. A study reported that Fos Proto-Oncogene (FOS) was related to cardiac fibrosis and inflammation[20]. Hypochlorite modified albumin (ALB) is an active compound that is formed during the reaction between proteins, and was found to be much higher in concentration and to act as a mediator of oxidative stress and inflammation in patients with uremia or diabetes mellitus[21]. These results show that the 6 hub genes might act as vital roles in the pathological of DN.

It is of interest that neutrophils decreased drastically in DN patients, which is in contrast to the study of an STZ (streptozotocin) induced diabetic mouse model[22]. There are several possible reasons for this opposite conclusion: (1) the negative feedback regulation of the immune microenvironment; (2) the impact of intervention drugs may exert anti-inflammatory activities, independent of their hemodynamic effects[23]. (3) the sample size of this study is still not enough, resulting in abnormal results. (4) neutrophils may have been transformed into other immune cells.

Nevertheless, some limitations still existed in our study: first, the infiltration of immune cells was estimated by algorithm, not traditional measurement method; second, the exact mechanism of hub genes had not been investigated in the present study. So, there is an urgent need to conduct in vivo experiments to confirm the results with higher-level evidence.

# Conclusions

In conclusion, our work provides a global picture of the immune environment in the glomerulus of DN. The potential therapeutic targets identified in the present study may provide new insightful for clinical treatment.

# Abbreviations

**DN:** Diabetic nephropathy; **DEGs:** Differentially expressed genes; **GEO:** Gene Expression Omnibus; **GO:** Gene Ontology; **KEGG:** Kyoto Encyclopedia of Genes and Genomes. **PCA:** Principal component analysis; **GSEA:** Gene set enrichment analysis; **STRING:** Search Tool for the Retrieval of Interacting Genes; **eGFR:** estimated glomerular filtration rate.

# Declarations

- Ethics approval and consent to participate

Not applicable

- Consent for publication

Not applicable.

- Availability of data and materials

All raw data are available in GEO datasets (GSE96804, GSE30528, and GSE1009).

- Competing interests

The authors declare that they have no competing interests.

- Funding

Not applicable.

- Authors' contributions

Wei ZHOU performed this research, created the figures and tables, and wrote the manuscript. Yaoyu LIU and Qinghong HU helped to revise the original manuscript. Junbiao WU provided the interpretation of the raw data. Hua LIN and Jiuyao ZHOU designed the research, provided the final critical revisions and conceptual support. All authors read and approved the final manuscript.

- Acknowledgements

Not applicable.

# References

1. Reutens AT: **Epidemiology of diabetic kidney disease.***Med Clin North Am* 2013, **97:**1-18.
2. Breyer MD, Susztak K: **The next generation of therapeutics for chronic kidney disease.***Nat Rev Drug Discov* 2016, **15:**568-588.
3. Fineberg D, Jandeleit-Dahm KA, Cooper ME: **Diabetic nephropathy: diagnosis and treatment.***Nat Rev Endocrinol* 2013, **9:**713-723.
4. Guiteras R, Sola A, Flaquer M, Manonelles A, Hotter G, Cruzado JM: **Exploring macrophage cell therapy on Diabetic Kidney Disease.***J Cell Mol Med* 2019, **23:**841-851.
5. Bending JJ, Lobo-Yeo A, Vergani D, Viberti GC: **Proteinuria and activated T-lymphocytes in diabetic nephropathy.***Diabetes* 1988, **37:**507-511.
6. Xiao X, Ma B, Dong B, Zhao P, Tai N, Chen L, et al: **Cellular and humoral immune responses in the early stages of diabetic nephropathy in NOD mice.***J Autoimmun* 2009, **32:**85-93.

7. Okon K, Stachura J: **Increased mast cell density in renal interstitium is correlated with relative interstitial volume, serum creatinine and urea especially in diabetic nephropathy but also in primary glomerulonephritis.***Pol J Pathol* 2007, **58:**193-197.
8. Galkina E, Ley K: **Leukocyte recruitment and vascular injury in diabetic nephropathy.***J Am Soc Nephrol* 2006, **17:**368-377.
9. Newman AM, Liu CL, Green MR, Gentles AJ, Feng W, Xu Y, et al: **Robust enumeration of cell subsets from tissue expression profiles.***Nat Methods* 2015, **12:**453-457.
10. Benito M, Parker J, Du Q, Wu J, Xiang D, Perou CM, et al: **Adjustment of systematic microarray data biases.***Bioinformatics* 2004, **20:**105-114.
11. **limma powers differential expression analyses for RNA-sequencing and microarray studies.***Nucleic Acids Res* 2015, **43:**e47.
12. Chin CH, Chen SH, Wu HH, Ho CW, Ko MT, Lin CY: **cytoHubba: identifying hub objects and sub-networks from complex interactome.***BMC Syst Biol* 2014, **8 Suppl 4:**S11.
13. Yuan WH, Xie QQ, Wang KP, Shen W, Feng XF, Liu Z, et al: **Screening of osteoarthritis diagnostic markers based on immune-related genes and immune infiltration.***Sci Rep* 2021, **11:**7032.
14. Tan L, Xu Q, Shi R, Zhang G: **Bioinformatics analysis reveals the landscape of immune cell infiltration and immune-related pathways participating in the progression of carotid atherosclerotic plaques.***Artif Cells Nanomed Biotechnol* 2021, **49:**96-107.
15. Wang L, Wei Q, Zhang M, Chen L, Li Z, Zhou C, et al: **Identification of the prognostic value of immune gene signature and infiltrating immune cells for esophageal cancer patients.***Int Immunopharmacol* 2020, **87:**106795.
16. Betz BB, Jenks SJ, Cronshaw AD, Lamont DJ, Cairns C, Manning JR, et al: **Urinary peptidomics in a rodent model of diabetic nephropathy highlights epidermal growth factor as a biomarker for renal deterioration in patients with type 2 diabetes.***Kidney Int* 2016, **89:**1125-1135.
17. Cui S, Zhu Y, Du J, Khan MN, Wang B, Wei J, et al: **CXCL8 Antagonist Improves Diabetic Nephropathy in Male Mice With Diabetes and Attenuates High Glucose-Induced Mesangial Injury.***Endocrinology* 2017, **158:**1671-1684.
18. Panee J: **Monocyte Chemoattractant Protein 1 (MCP-1) in obesity and diabetes.***Cytokine* 2012, **60:**1-12.
19. Chow FY, Nikolic-Paterson DJ, Ozols E, Atkins RC, Rollin BJ, Tesch GH: **Monocyte chemoattractant protein-1 promotes the development of diabetic renal injury in streptozotocin-treated mice.***Kidney Int* 2006, **69:**73-80.
20. Palomer X, Roman-Azcona MS, Pizarro-Delgado J, Planavila A, Villarroya F, Valenzuela-Alcaraz B, et al: **SIRT3-mediated inhibition of FOS through histone H3 deacetylation prevents cardiac fibrosis and inflammation.***Signal Transduct Target Ther* 2020, **5:**14.
21. Tang DD, Niu HX, Peng FF, Long HB, Liu ZR, Zhao H, et al: **Hypochlorite-Modified Albumin Upregulates ICAM-1 Expression via a MAPK-NF-kappaB Signaling Cascade: Protective Effects of Apocynin.***Oxid Med Cell Longev* 2016, **2016:**1852340.

22. Mohamed R, Jayakumar C, Ranganathan PV, Ganapathy V, Ramesh G: **Kidney proximal tubular epithelial-specific overexpression of netrin-1 suppresses inflammation and albuminuria through suppression of COX-2-mediated PGE2 production in streptozotocin-induced diabetic mice.***Am J Pathol* 2012, **181:**1991-2002.
23. Mizuno M, Sada T, Kato M, Fukushima Y, Terashima H, Koike H: **The effect of angiotensin II receptor blockade on an end-stage renal failure model of type 2 diabetes.***J Cardiovasc Pharmacol* 2006, **48:**135-142.

# Figures

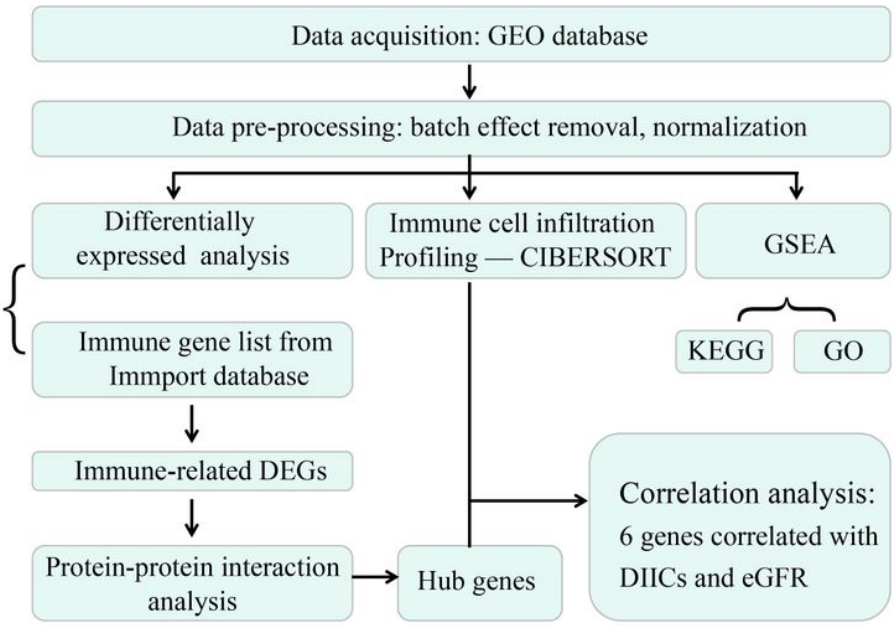


**Figure 1**

Flowchart of this study. DEGs: differentially expressed genes; CIBERSORT: cell-type identification by estimating relative subsets of RNA transcripts; DIICs: differentially infiltrated immune cells; GO: Gene Ontology; KEGG: Kyoto Encyclopedia of Genes and Genomes; GSEA: Gene set enrichment analysis; eGFR: estimated glomerular filtration rate.

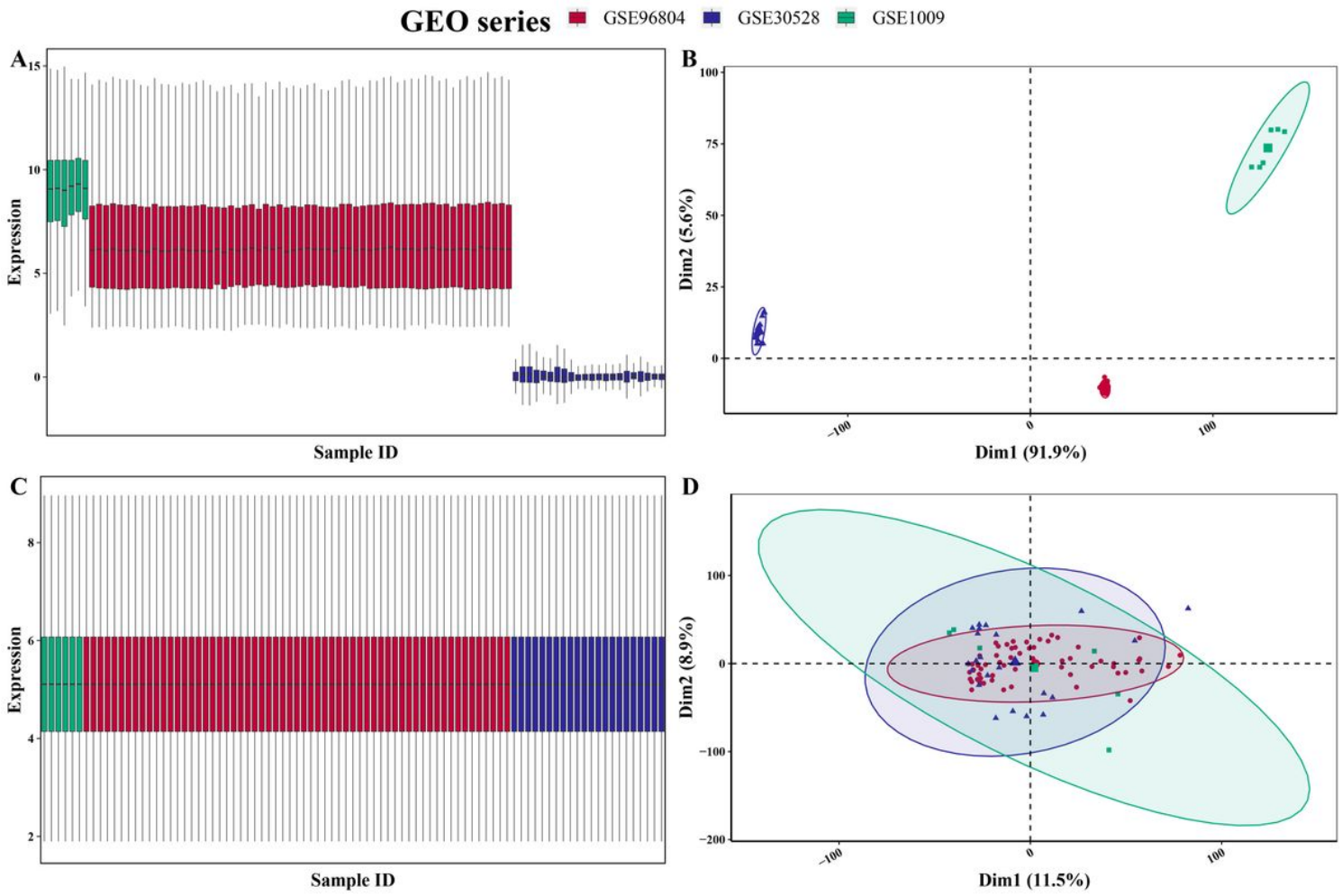


## Figure 2

Batch effect removement and data normalization. (A-B) Box and PCA plot of three GEO series before removal of batch effect and data normalization. (C-D) Box and PCA plot of three GEO series after removal of batch effect and data normalization.

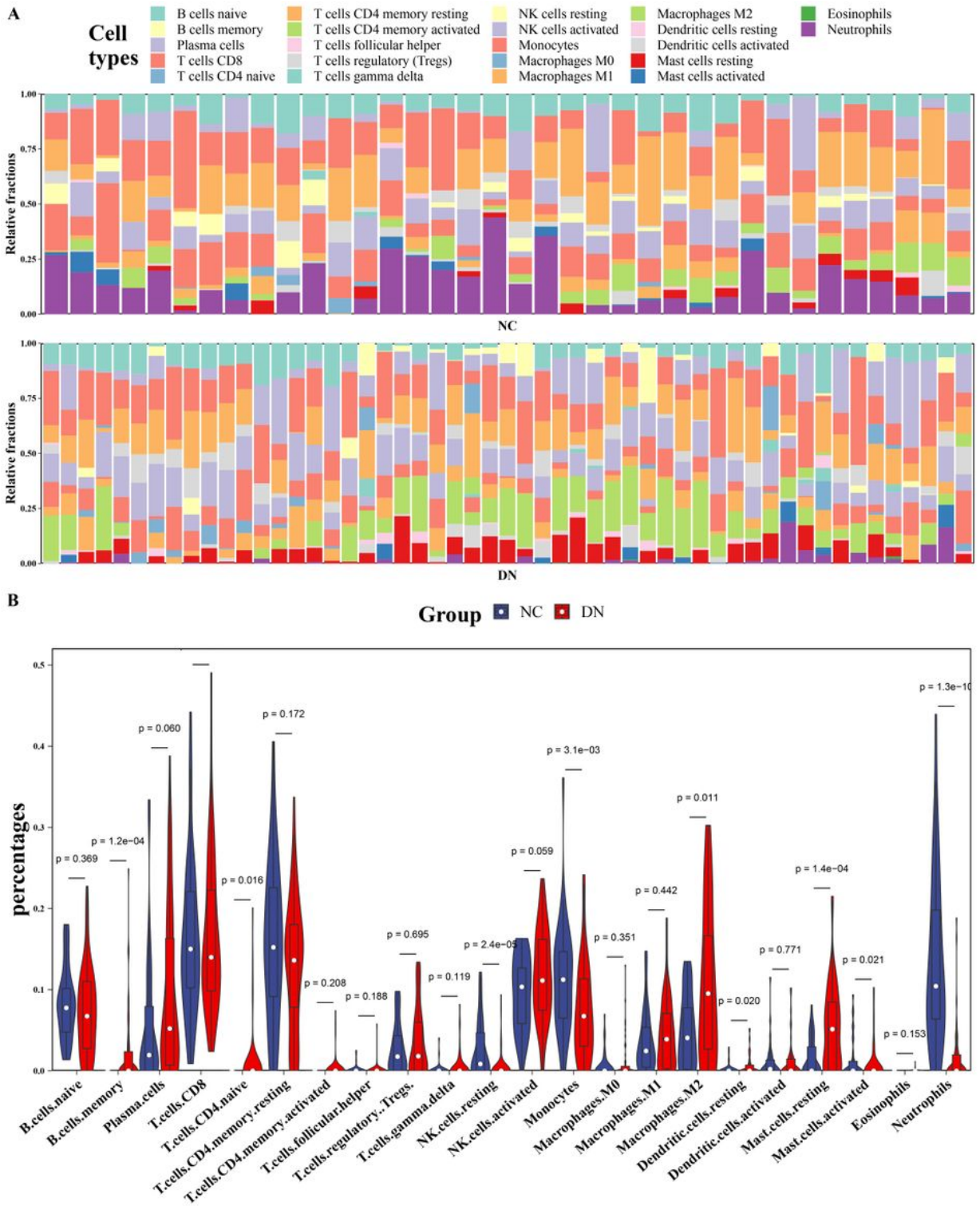


## Figure 3

Analysis of immune cell infiltration by the CIBERSORT algorithm. (A) Stacked bar plot shows the relative percent of 22 types of immune cell in each sample of two groups. (B) Violin plot shows the differences of immune infiltration between two groups.

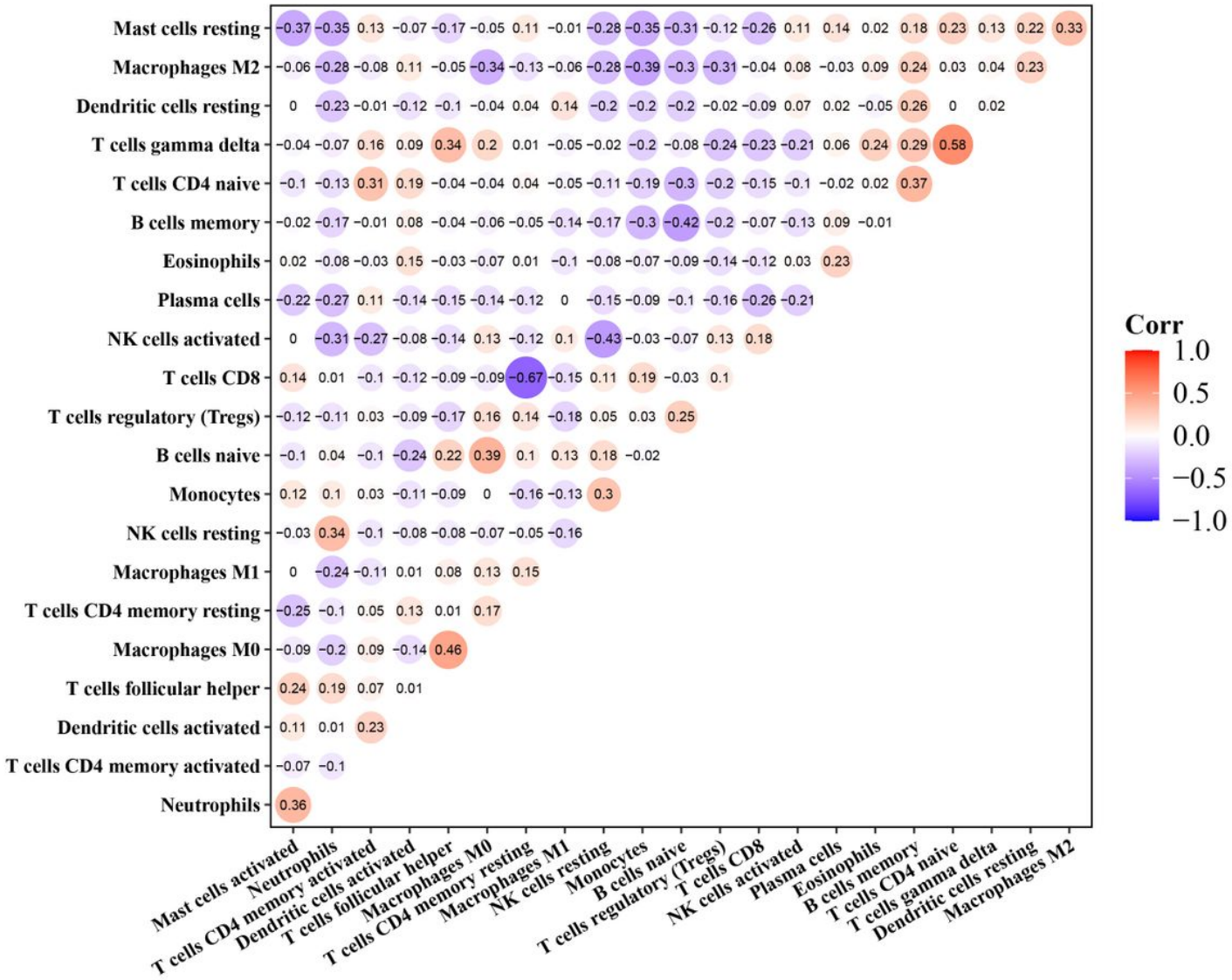


## Figure 4

Correlation analysis of 22 types of immune cells. Red: positive correlation; blue: negative correlation.

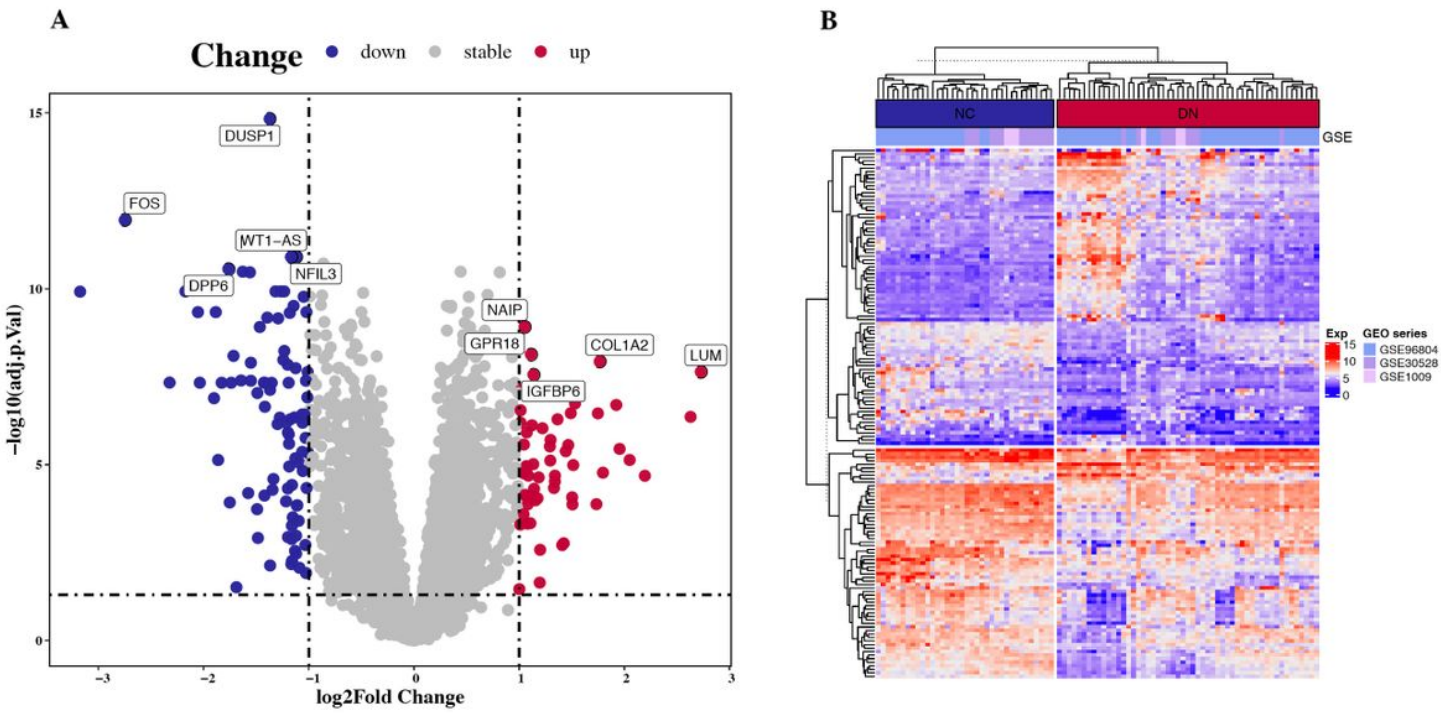


## Figure 5

Differential gene expression analysis for DN vs. NC. (A) Volcano plot of dysregulated genes (|log2FC (fold change) | > 1 and adjusted P-value < 0.05). Blue points represent relatively downregulated genes, red points represent upregulated genes, gray points represent genes showing no significant alteration. (B) Heatmap of the 149 DEGs expression level among 89 samples.

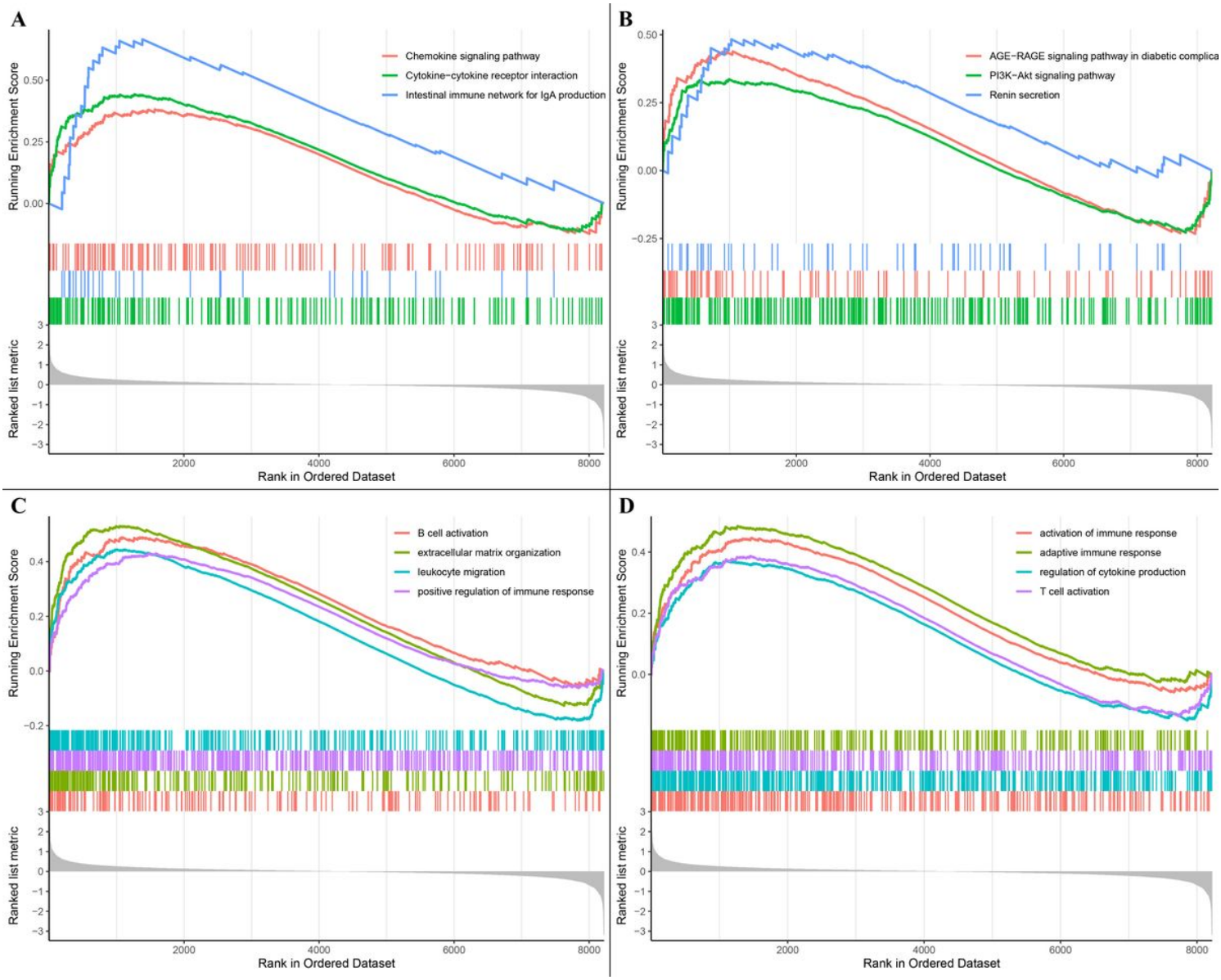


## Figure 6

Results of KEGG and GO by the GSEA method. (A) 3 representative enriched immune-related KEGG pathways. (B) 3 representative enriched DN-related KEGG pathways. (C-D) 8 representative enriched immune related GO gene sets. GSEA: Gene set enrichment analysis; KEGG: Kyoto Encyclopaedia of Genes and Genomes; GO: gene ontology.

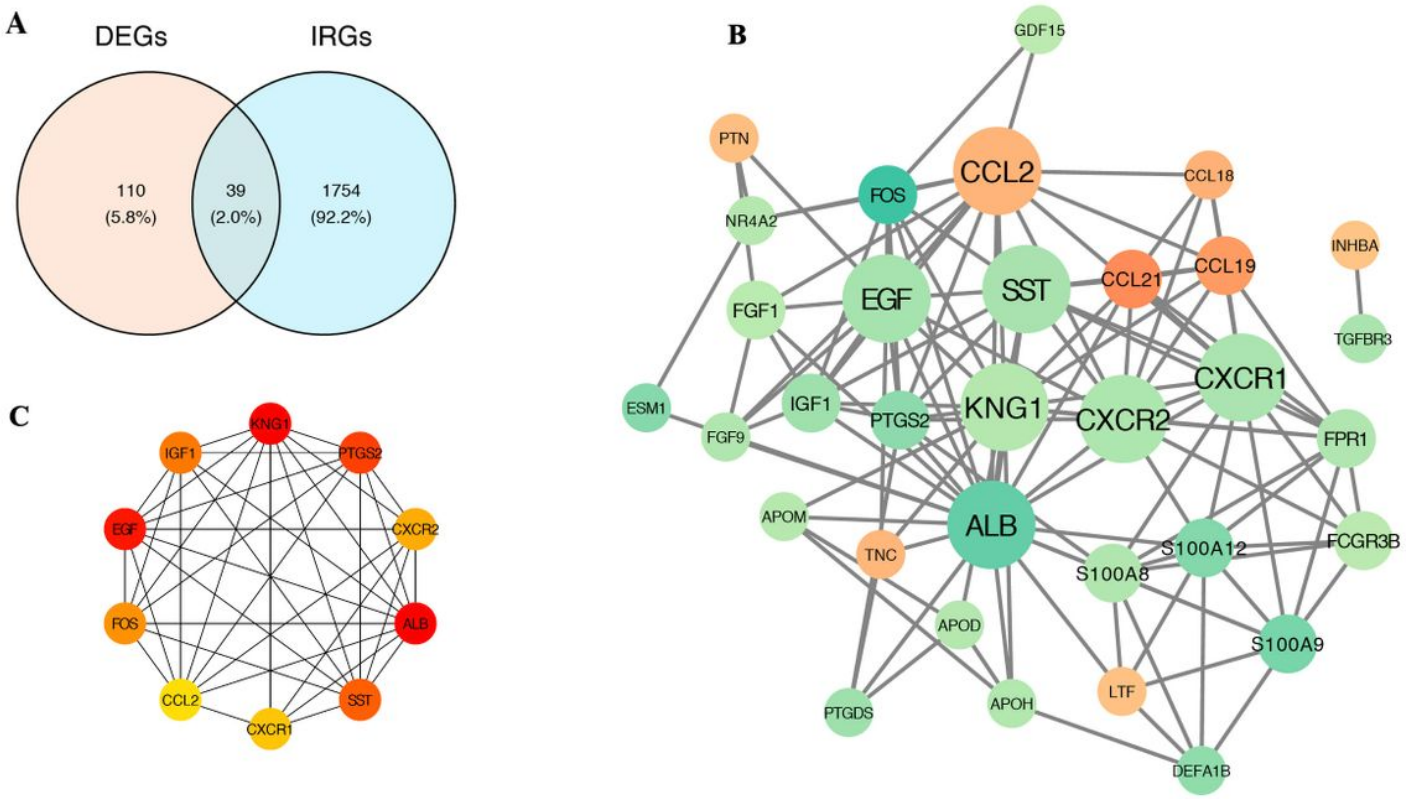


## Figure 7

PPI network construction of Immune-related DEGs. (A) The intersection of 149 DEGs with 1793 immune-related gene from the Immport database. (B) PPI of immune-related DEGs (The node size indicates the clustering coefficient, a larger size indicated a larger clustering coefficient; The node color indicates the log2FC of DEGs, orange represents up regulated genes, while green represents down regulated genes). (C) hub gene identified by the Maximum clique centrality (MCC) algorithm using the “Cytohubba” plug-in. IRGs: immune related genes from the Immport database.

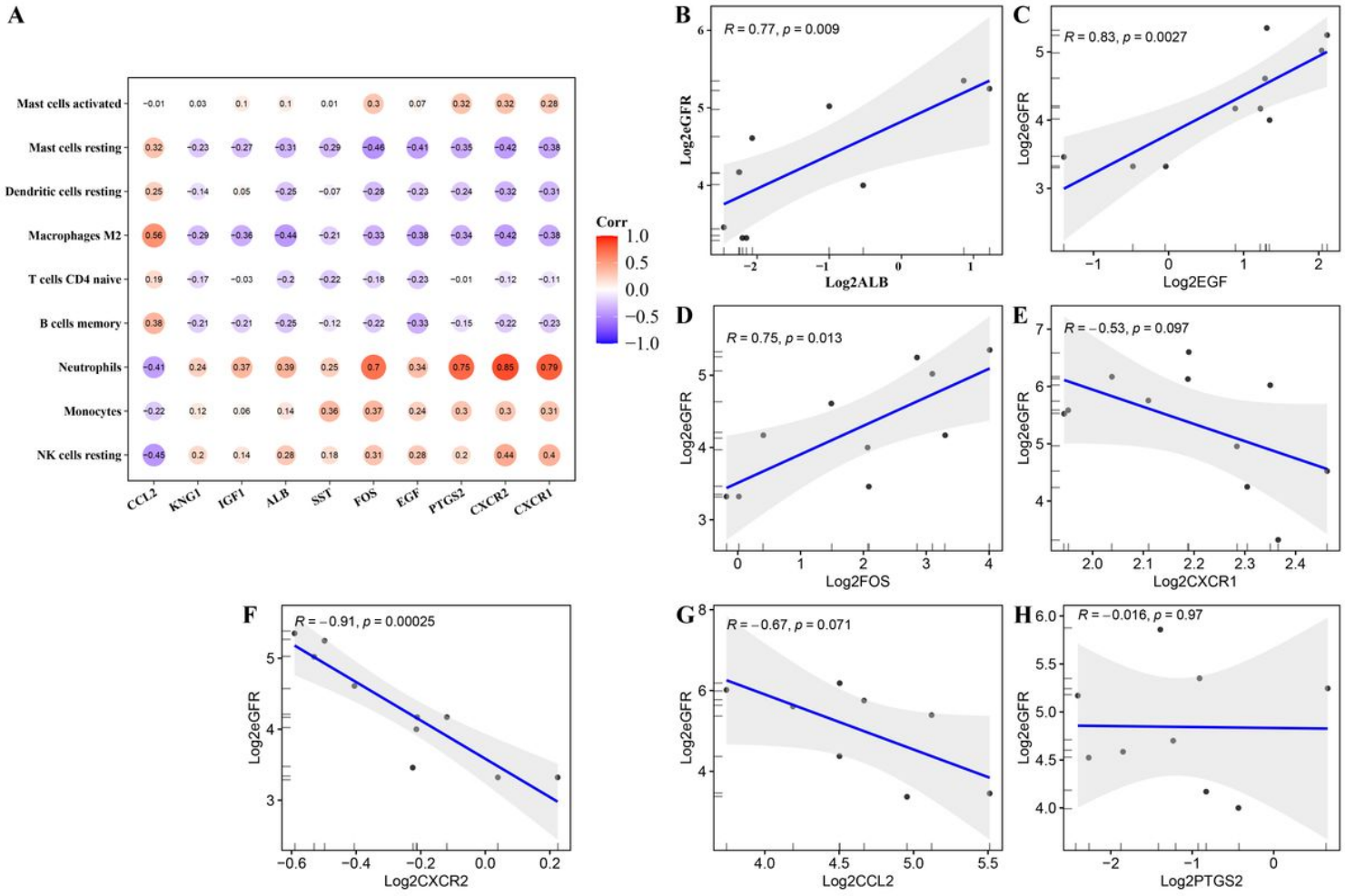


## Figure 8

Correlation analysis of hub genes with infiltrated immune cells and eGFR. (A) Correlation heat map between hub genes and differently infiltrated immune cells. (B-H) Correlation analysis of hub genes and eGFR.